



## Early Pleistocene occurrence of Acheulian technology in North China

Xingwen Li<sup>a, b</sup>, Hong Ao<sup>a, c, \*</sup>, Mark J. Dekkers<sup>d</sup>, Andrew P. Roberts<sup>e</sup>, Peng Zhang<sup>a, b</sup>,  
Shan Lin<sup>a, b</sup>, Weiwen Huang<sup>f</sup>, Yamei Hou<sup>f</sup>, Weihua Zhang<sup>g</sup>, Zhisheng An<sup>a</sup>

<sup>a</sup> State Key Laboratory of Loess and Quaternary Geology, Institute of Earth Environment, Chinese Academy of Sciences, Xi'an 710061, China

<sup>b</sup> University of Chinese Academy of Sciences, Beijing 100049, China

<sup>c</sup> Lamont-Doherty Earth Observatory, Columbia University, Palisades, New York 10964, United States

<sup>d</sup> Paleomagnetic Laboratory 'Fort Hoofddijk', Department of Earth Sciences, Faculty of Geosciences, Utrecht University, Budapestlaan 17, 3584 CD Utrecht, The Netherlands

<sup>e</sup> Research School of Earth Sciences, The Australian National University, Canberra 2601, Australia

<sup>f</sup> Key Laboratory of Vertebrate Evolution and Human Origin of Chinese Academy of Sciences, Institute of Vertebrate Paleontology and Paleoanthropology, Chinese Academy of Sciences, Beijing 100044, China

<sup>g</sup> Henan Museum, Zhengzhou 450002, China

## ARTICLE INFO

## Article history:

Received 18 April 2016

Received in revised form

3 November 2016

Accepted 21 November 2016

Available online 30 November 2016

## Keywords:

Magneto-cyclostratigraphy

Chinese loess-paleosol sequence

Acheulian technology

Early Pleistocene

Sanmenxia Basin

North China

## ABSTRACT

Acheulian tools with their associated level of cognizance heralded a major threshold in the evolution of hominin technology, culture and behavior. Thus, unraveling occurrence ages of Acheulian technology across different regions worldwide constitutes a key aspect of understanding the archeology of early human evolution. Here we present a magneto-cyclochronology for the Acheulian assemblage from Sanmenxia Basin, Loess Plateau, North China. Our results place a sequence of stable normal and reversed paleomagnetic polarities within a regional lithostratigraphic context. The Acheulian assemblage is dated to be older than the Matuyama–Brunhes boundary at 0.78 Ma, and is found in strata that are probably equivalent to a weak paleosol subunit within loess layer L<sub>9</sub> in the Chinese loess-paleosol sequence, which corresponds to marine isotope stage (MIS) 23, a relatively subdued interglacial period with age range of ~0.89–0.92 Ma. This age of ~0.9 Ma implies that Acheulian stone tools were unambiguously present in North China during the Early Pleistocene. It distinctly enlarges the geographic distribution of Acheulian technology and brings its occurrence in North China back into the Early Pleistocene, which is contemporaneous with its first emergence in Europe. Combined with other archeological records, the larger area over which Acheulian technology existed in East Asia during the terminal Early Pleistocene has important implications for understanding early human occupation of North China.

© 2016 Elsevier Ltd. All rights reserved.

## 1. Introduction

Acheulian technology is characterized by bifacially and unifacially shaped tool types, such as handaxes, cleavers, picks and other large cutting tools (LCTs) (Isaac, 1969; Bar-Yosef and Goren-Inbar, 1993; Goren-Inbar et al., 2000; Semaw et al., 2009; Lepre et al., 2011; Beyene et al., 2013; Diez-Martín et al., 2015). Its appearance represents a technological advance over the preceding Oldowan technology, and is associated with innovative hominin cognitive and adaptive abilities (Goren-Inbar, 2011; Stout, 2011). Current thinking is that Acheulian technology originated in East

Africa (possibly West Turkana, Kenya) at least 1.76 million years ago (Ma) (Lepre et al., 2011), that it became distributed somewhat widely across Africa (e.g., Vaal River Valley and Gona) at ~1.6 Ma (Gibbon et al., 2009; Semaw et al., 2009), and then spread to the Levant at ~1.4 Ma (Bar-Yosef and Goren-Inbar, 1993), South Asia at 1.5–1.1 Ma (Pappu et al., 2011), and Europe at 1.0–0.9 Ma (Scott and Gibert, 2009; Vallverdú et al., 2014) (Fig. 1). The 0.8–0.9 Ma Acheulian stone tools from South and central China (Hou et al., 2000; de Lumley and Li, 2008) (Fig. 1) suggest that Acheulian technology arose in China at least during the terminal Early Pleistocene. However, there are only a few sites with *in situ* Acheulian artefacts from North China with ages ranging from the late Mid-Pleistocene to the Late Pleistocene (Wang et al., 2014; Yang et al., 2014) (Fig. 1). Thus, it remains enigmatic as to how early Acheulian technology can be traced back in North China, compared with

\* Corresponding author. State Key Laboratory of Loess and Quaternary Geology, Institute of Earth Environment, Chinese Academy of Sciences, Xi'an 710061, China.  
E-mail address: [aohong@ieecas.cn](mailto:aohong@ieecas.cn) (H. Ao).

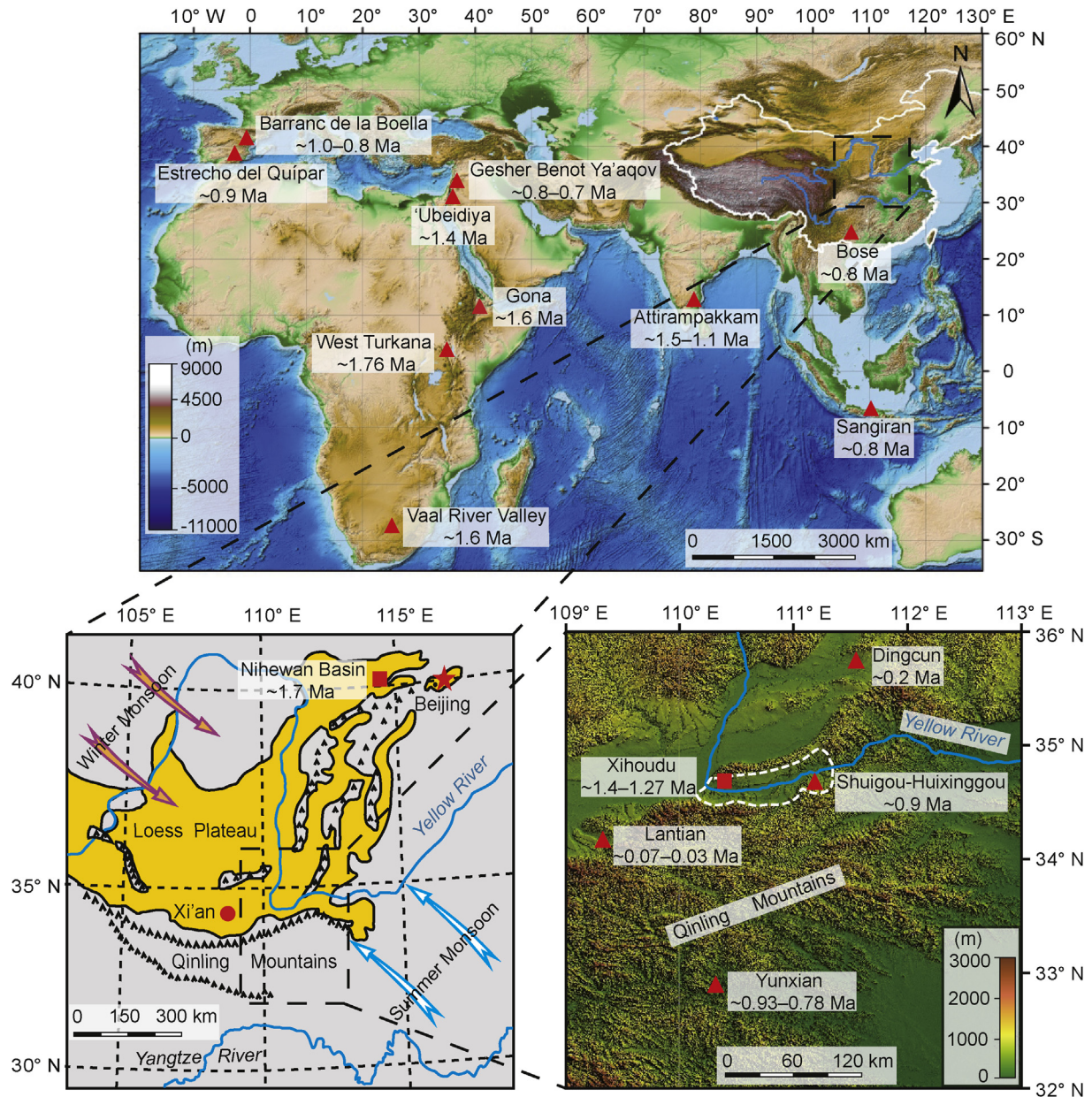


**Fig. 1.** Topographic map with locations of the Shuigou-Huixinggou site in the Sanmenxia Basin (dashed white lines) and other Paleolithic sites mentioned in the text. The red triangles and squares represent the Paleolithic sites that are characterized by Acheulian and Oldowan technologies, respectively, with ages for West Turkana from Lepre et al. (2011), Vaal River Valley from Gibbon et al. (2009), Gona from Semaw et al. (2009), Estrecho del Quípar from Scott and Gibert (2009), Barranc de la Boella from Vallverdú et al. (2014), 'Ubeidiya from Bar-Yosef and Goren-Inbar (1993), Gesher Benot Ya'aqov from Goren-Inbar et al. (2000), Attirampakkam from Pappu et al. (2011), Sangiran from Simanjuntak et al. (2010), Bose from Hou et al. (2000), Nihewan Basin from Zhu et al. (2004) and Ao et al. (2013b), Yunxian from de Lumley and Li (2008), Xihoudu from Zhu et al. (2003) and Kong et al. (2013), Lantian from Wang et al. (2014) and Dingcun from Yang et al. (2014).

its Early Pleistocene occurrence in South and central China.

Sanmenxia Basin (also Sanmen area), which lies on the south-eastern Loess Plateau, is a rich source of stone artefacts and is an important area for understanding the early human occupation of North China (Jia et al., 1961; Huang, 1964; Jia, 1985; Li, 1990). The first Early Pleistocene Paleolithic site in China, that is the Xihoudu site dated at 1.4–1.27 Ma (Zhu et al., 2003; Kong et al., 2013), was found in northwestern Sanmenxia Basin (Fig. 1) in 1961–1962 (Jia, 1985). In 1963, 128 stone artefacts were found from 6 localities in eastern Sanmenxia Basin (Huang, 1964). Among the 128 artefacts, 94 were from the Shuigou and Huixinggou sites (Huang, 1964). At that time the chronology of the Chinese loess-paleosol sequence

was not yet established; a tentative Mid-Pleistocene age was suggested for the lithic assemblage based on lithostratigraphic arguments (Huang, 1964). Furthermore, when these artefacts were discovered, consensus was that Acheulian handaxes and cleavers were lacking in East Asia during the period when they flourished in Africa and western Eurasia (Movius, 1948). Therefore, the handaxe and cleavers from the Shuigou and Huixinggou sites (Fig. 2) were not recognized and reported as Acheulian artefacts; instead, they were considered to represent different kinds of choppers that are indicative of a chopper-chopping tool industry (Huang, 1964, 1987, 1993; Lin, 1992).

In the present study, we reassess the previously excavated lithic



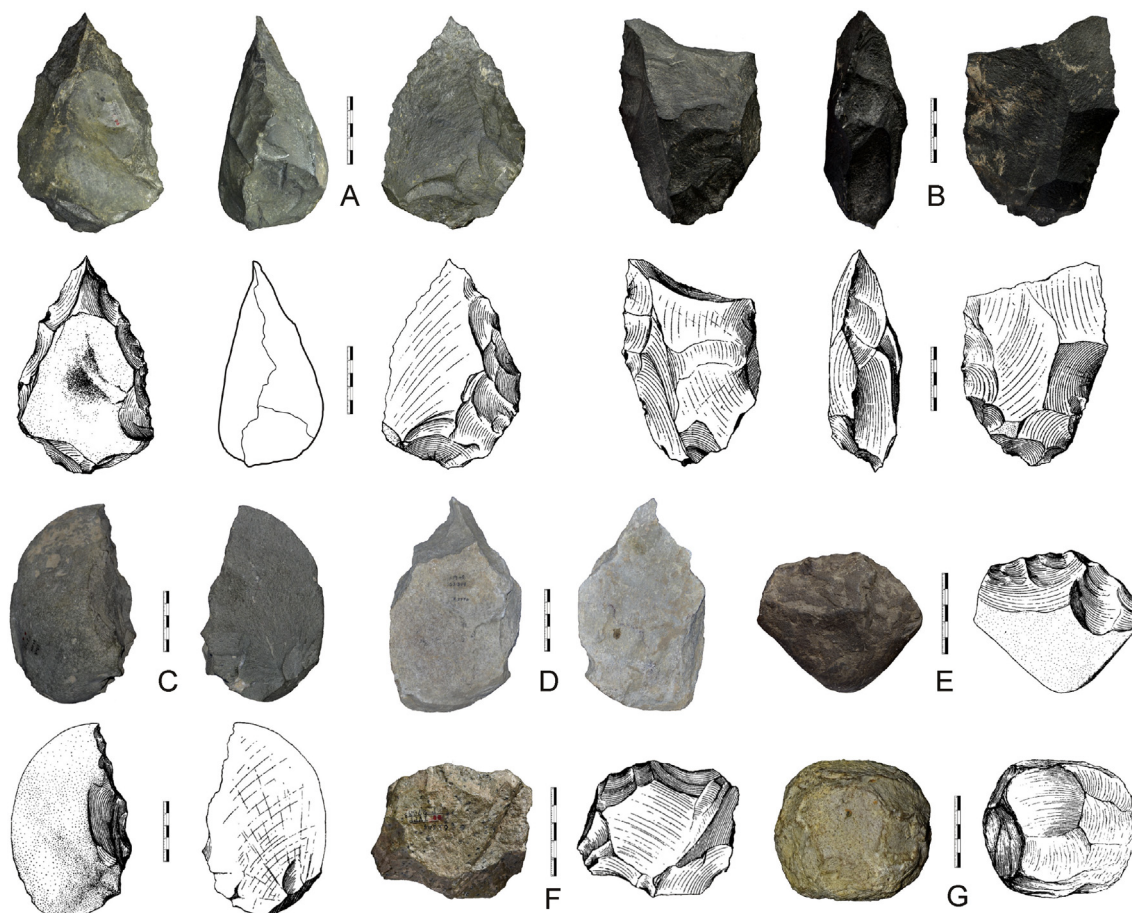


**Fig. 2.** Characteristic *in situ* artefacts from the Shuigou-Huixinggou site in the Sanmenxia Basin. Artefacts include: (A) handaxe (P. 2768); (B) cleaver (P. 2769); (C) cleaver (P. 2752); (D) pick (P. 2770); (E) unifacial chopper (P. 2758); (F) bifacial chopper (P. 2763); and (G) spheroid (P. 2774). The line drawings of artefacts are after Huang (1964). (Scale bars: 5 cm).

assemblage from the Shuigou and Huixinggou sites. We establish a numerical age for the lithic assemblage using magneto-cyclostratigraphy. We provide definitive evidence of an Early Pleistocene date for Acheulian stone tools in North China, which offers an important new window into the distribution of Acheulian technology out of Africa during the late Early Pleistocene.

## 2. General setting

The Loess Plateau is situated near the middle reaches of the Yellow River in North China (Fig. 1). It hosts a vast expanse (~300,000 km<sup>2</sup>) of thick eolian dust deposits, which are among the world's most outstanding terrestrial archives of Late Cenozoic climatic and environmental changes (Liu, 1985). Sanmenxia Basin is an intermontane basin in the southeastern Loess Plateau, through which the Yellow River flows from west to east (Fig. 1). The east-west trending Qinling Mountains are situated south of the basin, and form the boundary between temperate and semi-arid North China and subtropical and humid South China in terms of climate, fauna and flora (Zhu et al., 2015). Generally, the loess-paleosol sequence in this basin is underlain by fluvial-lacustrine sediments, the so-called Sanmen Formation (Young and Pei, 1933; Liu, 1985; Wang et al., 2004). At present, the basin has a temperate monsoon climate with annual precipitation of 500–700 mm and a mean annual temperature of 12–14 °C. More than 60% of precipitation is in the summer.

The Shuigou and Huixinggou sites are located in eastern Sanmenxia Basin, on the southern bank of the Yellow River, ~5 km

northeast of Sanmenxia city (Fig. 1 and Fig. A.1). The two sites are less than 200 m away from each other (Fig. A.1). The stone artefacts were found from the same stratigraphic level at these two localities. The artefact layer can be traced in the field from Shuigou to Huixinggou; it consists of identical grayish-green fluvial silty clay that lies immediately above the lowermost conglomerate layer in the 4th terrace of the Yellow River. Thus, the localities have been merged into a single site that was initially named the Shuigou-Huixinggou site (Huang, 1964); while later on it was also known as the Sanmenxia site (Huang et al., 2005).

Our studied section is located at Huixinggou (34°47' N, 111°13' E, elevation 370 m), because it is better exposed and has a more complete stratigraphy than at Shuigou. The Huixinggou section is 103-m thick and can be divided into two portions: an overlying eolian Quaternary yellowish loess-paleosol sequence with underlying fluvial grayish-green silty clay and conglomerate (Young and Pei, 1933; Huang, 1964; Pan et al., 2005) (Fig. A.1). The loess-paleosol sequence has a thickness of 83 m (0 m represents the top of the section). The composite paleosol S<sub>5</sub> is a foremost marker layer in Chinese loess-paleosol sequences (Liu, 1985), and is clearly recognizable in the section. A thin conglomerate layer occurs at 75.4–76.1 m of the loess-paleosol sequence. Two conglomerate layers (83–85 m and 87.3–90.4 m) are intercalated with a fluvial silty clay layer (85–87.3 m) and are situated below the loess-paleosol sequence. The artefact layer occurs underneath the loess-paleosol sequence at around 95 m and in the middle of a grayish-green fluvial silty clay layer (90.4–100 m). The lowermost conglomerate layer below the artefact layer marks the onset of the

4th terrace of the Yellow River (Pan et al., 2005).

### 3. Sampling and analytical methods

To obtain samples that were as fresh as possible, surface outcrops (>20 cm) were removed to eliminate potential weathering effects. A total of 159 block samples that were oriented by magnetic compass were taken at 1 m intervals from the loess-paleosol sequence and at ~20–40 cm intervals from the fluvial sediments. Cubic specimens (2 cm × 2 cm × 2 cm) were subsequently obtained from the block samples in the laboratory for stepwise thermal demagnetization analysis. In addition, 4636 powdered samples were collected from the entire Huixinggou section for mass-specific magnetic susceptibility ( $\chi$ ) measurements, which are useful for establishing a time scale for the 83-m-thick loess-paleosol sequence.

$\chi$  was measured for the 4636 powdered samples with a Bartington Instruments MS2 magnetic susceptibility meter at 470 Hz. Four typical samples that represent the various lithologies and magnetic polarity zones of the Huixinggou section were selected for temperature-dependent susceptibility ( $\chi$ -T) and isothermal remanent magnetization (IRM) acquisition measurements. All  $\chi$ -T curves were measured from room temperature to 700 °C and back to room temperature in an argon atmosphere using a MFK1-FA Kappabridge with a CS-3 high-temperature furnace. Sample holder and thermocouple contributions to  $\chi$  were subtracted using the CUREVAL 5.0 program. IRM acquisition curves were determined with an ASC IM-10-30 pulse magnetizer up to 2.0 T and an AGICO JR-6A spinner magnetometer for remanence measurements. IRM acquisition curves consist of 31 IRM field steps.

Stepwise thermal demagnetization measurements for all block samples were conducted using a 2G Enterprises Model 755-R cryogenic magnetometer installed in a magnetically shielded laboratory (with ambient field < 300 nT). All samples were subjected to stepwise thermal demagnetization up to a maximum temperature of 680 °C with 20–50 °C increments using an ASC TD-48 thermal demagnetizer. After each demagnetization step, the remanent magnetization of each sample was measured. Demagnetization results were evaluated using orthogonal vector component diagrams (Zijderveld, 1967) and the principal component direction was computed using least-squares fitting (Kirschvink, 1980).

## 4. Results

### 4.1. Lithic assemblage

Most of the 94 stone artefacts were excavated *in situ* from fluvial silty clays at the Shuigou-Huixinggou site, although some were collected from the terrace surface (Huang, 1964). In addition, an upper premolar tooth of *Equus* sp. and fragments of the aquatic mollusk *Lamprotula* sp. were unearthed from this site. The surface-collected artefacts were likely washed down from the *in situ* artefact layer, because the distribution of surface-collected artefacts was strictly confined to the surface slope of the fluvial silty clay at or below the *in situ* artefact layer, and most of the artefacts were embedded in the fluvial silty clay. Also, similar to the *in situ* artefacts, sticky fluvial silty clay was generally adhered to the surface-collected artefacts. It is difficult to wash away, which suggests that they were formerly buried together in the same fluvial silty clay. Both *in situ* excavated and surface-collected artefacts are made of the same raw material with the same lithic technology. Therefore, it is reasonable to interpret that the surface-collected artefacts were also derived from the *in situ* artefact layer (Huang, 1964).

The lithic assemblage comprises retouched and trimmed LCTs,

including handaxes, cleavers, and picks; other artefacts include choppers, spheroids, cores and flakes (Huang, 1964, 1987, 1993; Lin, 1992). All the LCTs are made from large flake blanks. For example, a handaxe (Fig. 2A) is made on a large flake and is approximately symmetrical in planform and cross-section (Huang, 1987). Shaping mainly focuses on its distal end and lateral edges, rendering an elongated handaxe with a convergent tip and forceful cutting edges. The butt is moderately worked to be relatively thick and rounded. A U-shaped cleaver (Fig. 2B) has a broad cutting edge that is formed by two intersecting flake surfaces and is almost perpendicular to the long axis (Lin, 1992; Huang, 1993). Shaping occurs on both its lateral edges to reduce the cortical area. The butt is pointed and moderately worked. Another cleaver (Fig. 2C) is unifacially worked on one lateral edge, which is parallel to the long axis and would have been used as the butt (Lin, 1992; Huang, 1993). The other lateral edge is unmodified and would have been used as the cutting edge. The two lateral edges converge distally and form a pointed tip. A pick (Fig. 2D) has been shaped unifacially to form a trihedral cross-section with a sturdy and truncated tip, whilst its butt is slightly worked and thick. In addition, an unifacial chopper from an igneous pebble (Fig. 2E) and a bifacial chopper from an igneous flake (Fig. 2F) are shown, along with a well-rounded spheroid that could be considered as bola (Fig. 2G) (Huang, 1964). Cores for detachment of large flakes are lacking, which implies that these large flakes might have been procured elsewhere and were then transported to the studied site. The anvil technique was primarily used to prepare large flake blanks for LCTs, while direct hard-hammer percussion was the principal stone-knapping and tool-retouching technique (Huang, 1964).

### 4.2. Magnetic properties

All four  $\chi$ -T heating curves are characterized by a major  $\chi$  drop at about 585 °C (Fig. 3), which is consistent with the presence of magnetite. A steady  $\chi$  increase from room temperature to ~300 °C is possibly due to gradual unblocking of fine-grained ferrimagnetic particles (i.e., particles close to the superparamagnetic to stable single domain threshold size) (Deng et al., 2004, 2006; Liu et al., 2005). A subsequent  $\chi$  decrease at 300–500 °C is generally interpreted as due to conversion of ferrimagnetic maghemite to weakly magnetic hematite (Florindo et al., 1999; Zhu et al., 2001; Deng et al., 2004, 2006). Cooling curves for two loess/paleosol samples have much higher values than the corresponding heating curves, which indicates transformation of iron-containing clays or silicates to new ferrimagnetic mineral phase during heating above 600 °C (Hunt et al., 1995; Florindo et al., 1999; Zhu et al., 2001; Ao et al., 2009).

Consistent with the dominant contribution of magnetite to the magnetic mineralogy, all IRM acquisition curves undergo a major increase below 300 mT (Fig. 4). The additional slight increase in IRM after application of fields of >300 mT indicates the presence of high-coercivity hematite.

### 4.3. Magneto-cyclostratigraphy

The entire succession is devoid of suitable material for radiometric dating. Therefore, we carried out an integrated stratigraphic analysis, involving lithostratigraphy, magnetic susceptibility stratigraphy and magnetic polarity stratigraphy, to develop a robust age model for the succession along with an estimated age for the associated lithic assemblage. The loess-paleosol sequence and underlying fluvial silty clays have similar demagnetization behavior (Fig. 5). The natural remanent magnetization (NRM) generally has two components: (1) a secondary low-temperature component (LTC) isolated by progressive demagnetization to 150–250 °C

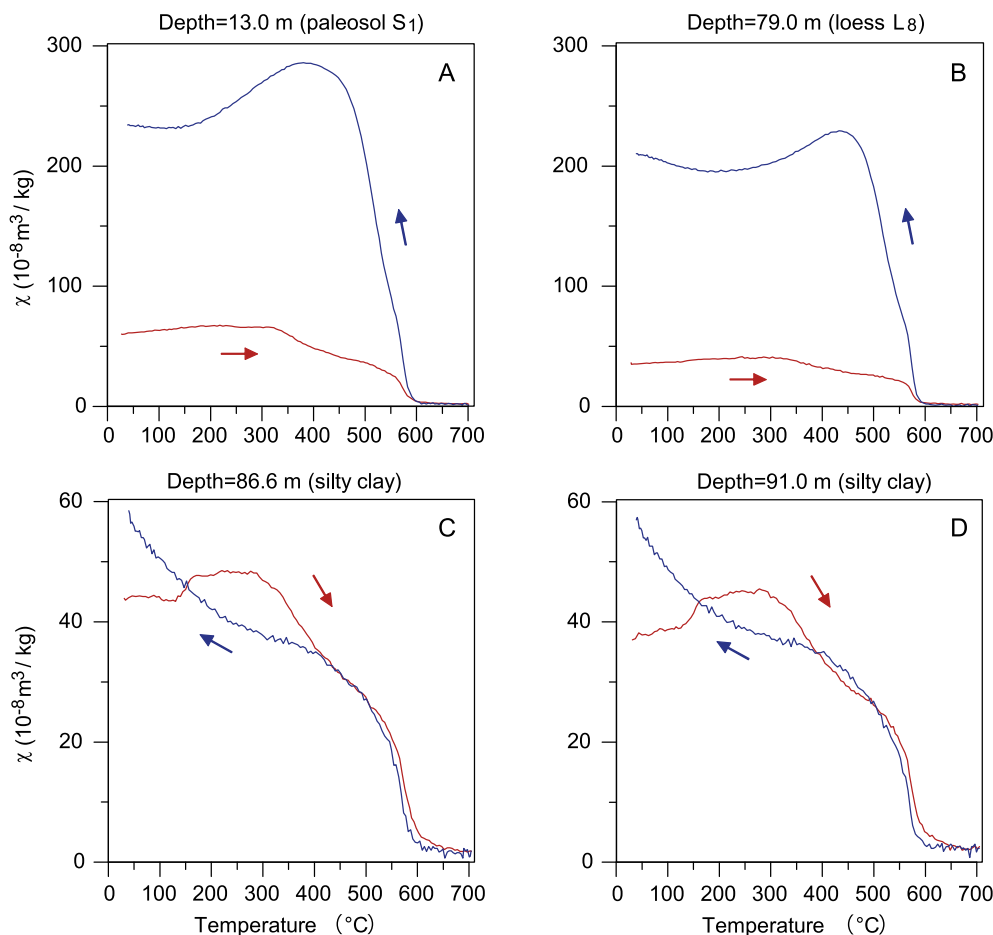


**Fig. 3.**  $\chi$ -T curves for four typical samples from the Huixinggou section. Red (blue) lines represent heating (cooling) curves. (For interpretation of the references to colour in this figure legend, the reader is referred to the web version of this article.)

(occasionally up to 400 °C) followed by (2) a characteristic remanent magnetization (ChRM) component isolated at higher temperatures (Fig. 5). The ChRM has a unidirectional trajectory trending toward the origin of orthogonal demagnetization plots. In contrast, the LTC does not decay toward the origin. The LTC has predominantly normal polarity and clusters around the present-day geomagnetic field (Fig. 6A). Strict criteria were used to determine ChRM directions: (1) data from at least four (but typically 8–15) consecutive demagnetization steps were used for linear fitting, starting at least at 250 °C, (2) a maximum angular deviation (MAD) < 10° was required for the line fit, and (3) a calculated virtual geomagnetic pole (VGP) latitude > 30° or < -30° (May and Butler, 1986; Ao et al., 2013a). Of the 159 sampled stratigraphic levels, samples from 112 levels (70%) meet these criteria (Table A.1). These 112 ChRM directions have a generally antipodal distribution with 65 normal and 47 reversed orientations (Fig. 6B). The 65 normal polarity ChRM directions have an overall mean with declination  $D = 2.5^\circ$  and inclination  $I = 48.2^\circ$  ( $k = 32$ ,  $\alpha_{95} = 3.2$ ;  $k$  is the precision parameter and  $\alpha_{95}$  is the radius of 95% confidence cone around the mean direction). The 47 reversed polarity ChRM directions have an overall mean of  $D = 190.1^\circ$  and  $I = -36.2^\circ$  ( $k = 14$ ,  $\alpha_{95} = 5.7$ ). The reversals test (McFadden and McElhinny, 1990) is negative, but this does not affect assignment of normal and reversed polarity. Finally, virtual geomagnetic pole (VGP) latitudes calculated from all of the 112 ChRM directions were used to develop a magnetostratigraphic polarity column for the studied sequence (Fig. 7). Two major polarity zones are recognized: a long normal polarity zone and an underlying relatively short reversed polarity

zone (Fig. 7).

Similar to the lithological variability,  $\chi$  variations for the Huixinggou section can be easily distinguished.  $\chi$  values for the loess-paleosol sequence range from  $\sim 40 \times 10^{-8} \text{ m}^3/\text{kg}$  in loess to over  $200 \times 10^{-8} \text{ m}^3/\text{kg}$  in some paleosols (Fig. 8A and B); such values are typical of Middle- and Late-Pleistocene loess-paleosol sequences from the Chinese Loess Plateau (Wang et al., 2005; Liu et al., 2015). The fluvial silty clays have similar  $\chi$  values as the overlying eolian loess layers, while sands within the conglomerate layers have higher  $\chi$  values than silty clay layers.

## 5. Discussion

### 5.1. Stratigraphic correlation and age estimation for the Shuigou-Huixinggou site

The chronological framework for the Chinese loess-paleosol sequence has been firmly established (Heller and Liu, 1982; Kukla et al., 1988; Porter and An, 1995; Liu et al., 2015). Orbital tuning of  $\chi$  (summer monsoon intensity proxy) and grain size (winter monsoon intensity proxy) records has enabled development of high-resolution age models over the last 2.6 Ma (Heslop et al., 2000; Ding et al., 2002; Sun et al., 2006). Generally, paleosol and loess layers with high and low  $\chi$  values, respectively, occurred during periods with strong and weak summer monsoon and corresponded to warm/humid interglacial and cold/dry glacial periods, respectively (Heller and Liu, 1982; Kukla et al., 1988). Lithological and  $\chi$  cycles for different loess-paleosol sequences across the Loess

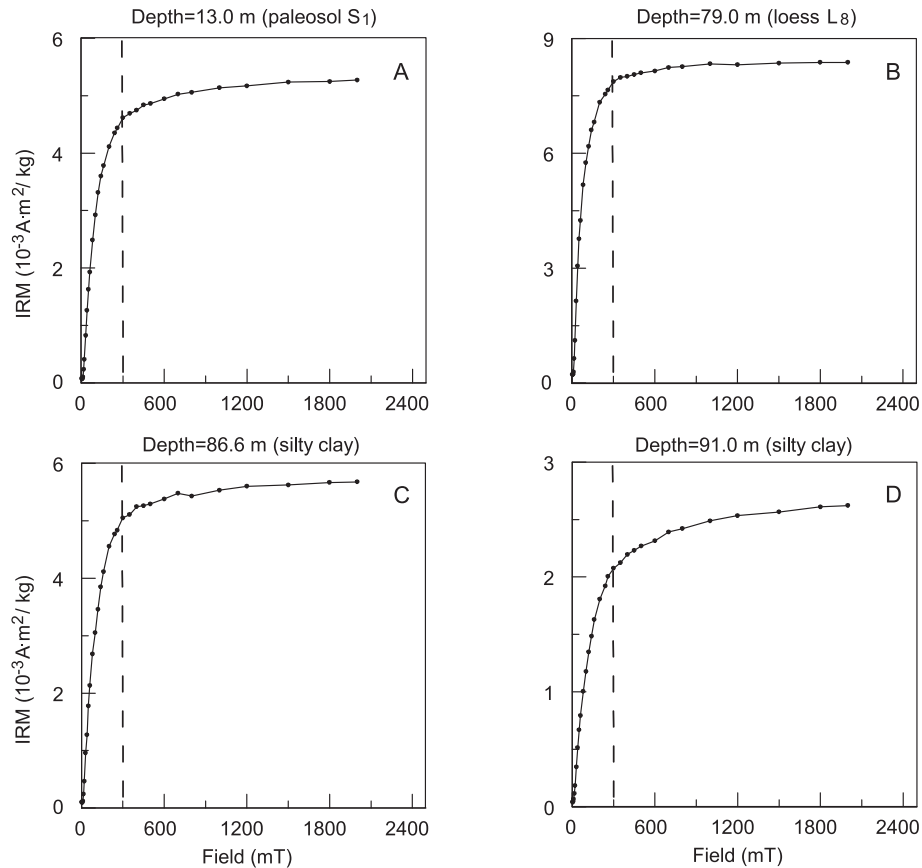


**Fig. 4.** Isothermal remanent Magnetization (IRM) acquisition curves for four typical samples from the Huixinggou section, the same levels as shown in Fig. 3. The dashed vertical lines at 300 mT are shown to differentiate between low- and high-coercivity portions of the IRM acquisition curves.

Plateau can be correlated from section to section and cycle-by-cycle to marine isotope stages (MIS) (Kukla and An, 1989; An et al., 1991; Heslop et al., 2000; Ding et al., 2002; Sun et al., 2006). At the Huixinggou section, both the lithological and  $\chi$  records for the 83-m-thick loess-paleosol sequence (Fig. 8A and B) can be correlated from  $S_0$  to upper  $S_8$  in the loess-paleosol sequences of the nearby Sanmenxia section (~20 km southwest of the Shuigou-Huixinggou site) and the Zhaojiachuan section (Fig. 8) (Wang et al., 2005; Sun et al., 2006). The artefact layer, which is situated below paleosol layer  $S_8$  at around 0.8 Ma (Sun et al., 2006; Liu et al., 2015), should, therefore, be older than 0.8 Ma.

Combining the established cyclostratigraphy for the upper loess-paleosol sequence from  $S_8$  to  $S_0$ , we can readily correlate the polarity sequence determined for the Huixinggou section to the geomagnetic polarity time scale (GPTS) (Hilgen et al., 2012). The normal (N1) and reversed (R1) polarity magnetozones are correlated to the Brunhes and upper Matuyama chrons, respectively (Fig. 8C and D). Consistent with paleomagnetic results from the Sanmenxia loess-paleosol succession (Wang et al., 2005), the Matuyama–Brunhes (M–B) boundary is located in uppermost paleosol unit  $S_8$  (Fig. 8A). Magnetozones R1 continues below paleosol unit  $S_8$ . Magnetozones R1 is thick and is likely to represent a sufficiently long period of time, which makes it highly unlikely to represent a short-duration geomagnetic excursion within the Brunhes chron (Roberts, 2008). Such an interpretation would also be at odds with the robust loess-paleosol sequence correlation. The artefact-bearing silty clay layer within magnetozones R1 is, therefore, unambiguously older than the M–B boundary. That is, it must be older than 0.78 Ma (Hilgen et al., 2012).

There are two potential age correlation options for the artefact layer (i.e., magnetozones R1) with the GPTS. The first relates it to the pre-Jaramillo Matuyama polarity chron. In this case, the post-Jaramillo Matuyama and Jaramillo polarity subchrons would be missing, which would indicate a sedimentary gap of more than 0.3 Myr. This would, in turn, result in an age >1.1 Ma for the artefact layer. However, the two conglomerate layers that overlie the artefact layer have no significant erosive base, which does not support the presence of a hiatus that would span from the Jaramillo subchron to the uppermost part of the Matuyama chron. On the Loess Plateau, including Sanmenxia Basin, termination of fluvial or lacustrine deposition would have been followed quickly by eolian deposition with only a small or even no sedimentary hiatus (Liu, 1985; Pan et al., 2005; Wang et al., 2005). If fluvial deposition had terminated in the pre-Jaramillo Matuyama chron, at least some loess-paleosol deposition would be expected during Jaramillo and post-Jaramillo Matuyama time (i.e., during the period from  $S_{12}$  to  $L_9$ ). These units are often more than 20-m thick in Sanmenxia Basin (Wang et al., 2005), but they are not exposed in this part of the terrace sequence in the Huixinggou section. Therefore, this pre-Jaramillo magnetostratigraphic correlation option is considered unlikely.

The second correlation option associates the artefact layer with the post-Jaramillo Matuyama chron (<0.99 Ma). In this case, there was only a small or no sedimentary hiatus between the eolian loess-paleosol sequence and the underlying fluvial gray-green silty clays and conglomerates. The two conglomerate layers that overlie the artefact layer merge gradually into one thicker conglomerate layer ~100 m to the west of the studied section, and the intercalated



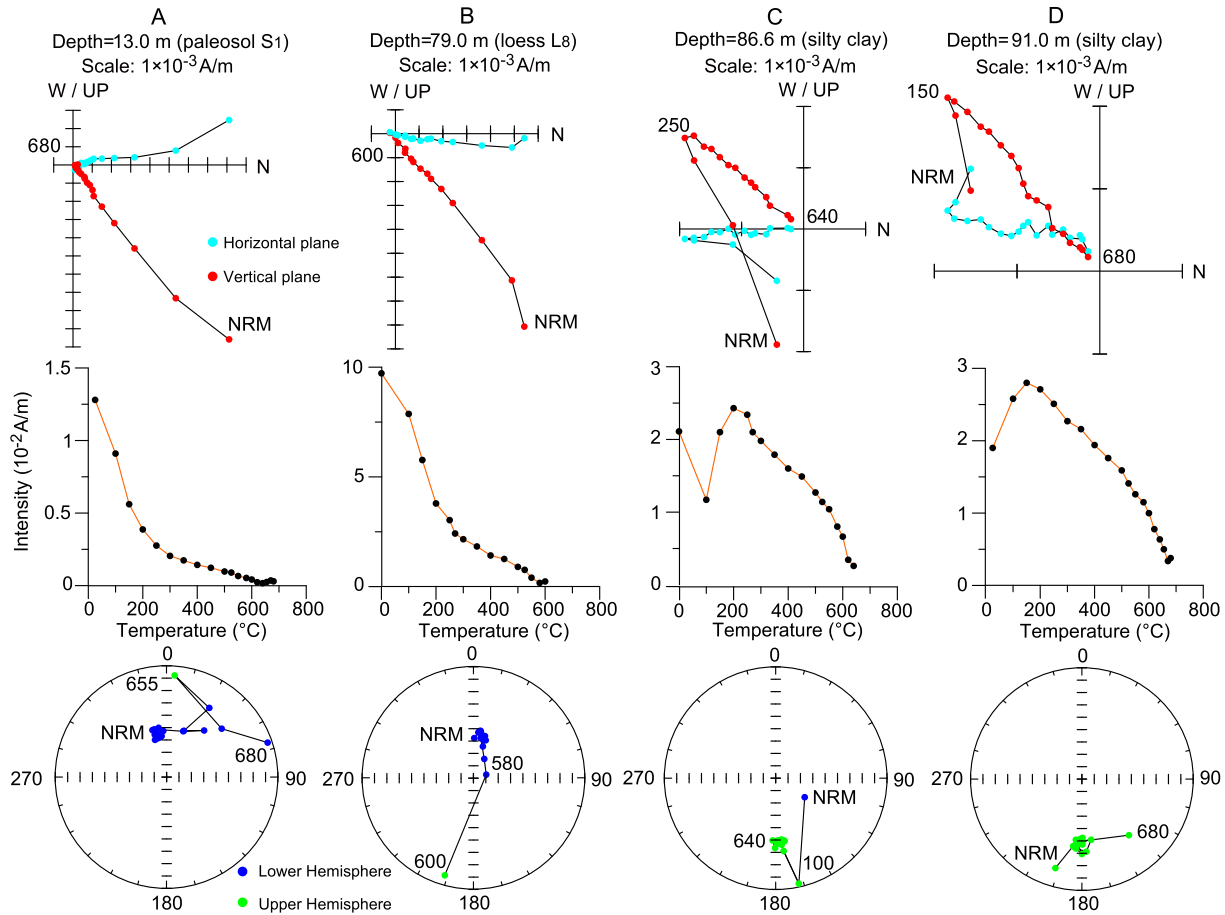


**Fig. 5.** The direction and intensity evolution of the NRM during stepwise thermal demagnetization for four typical samples from the Huixinggou section. Blue and red circles in the orthogonal projections represent horizontal and vertical planes, respectively. The numbers refer to the temperatures in °C. NRM is the natural remanent magnetization. (For interpretation of the references to colour in this figure legend, the reader is referred to the web version of this article.)

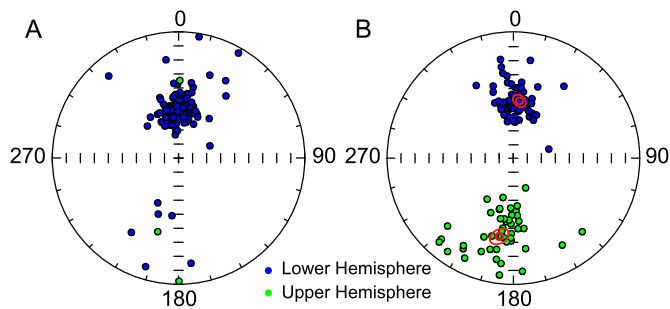


**Fig. 6.** (A) Equal area projections of paleomagnetic directions for 151 low-temperature remanent magnetization components and (B) 112 paleomagnetic directions of the high-temperature ChRM component for samples from the Huixinggou section. The red open circles in (B) represent the overall mean directions (with red ovals of 95% confidence cone) for both normal and reversed polarity samples. (For interpretation of the references to colour in this figure legend, the reader is referred to the web version of this article.)

silty clay layer that crops out in the Huixinggou section is not present, which makes a large time gap between the two conglomerate layers unlikely. Given that the overlying paleosol layer represents upper  $S_8$ , these two conglomerate layers (at 83–85 m and 87.3–90.4 m) could then correspond to high-energy fluvial deposition coeval with lower paleosol layer  $S_8$  or uppermost loess layer  $L_9$ . Relatively lower-energy deposition of the underlying silty clay layer may then have been coeval with loess layer  $L_9$ . Thus, the artefact layer with relatively higher  $\chi$  values in the middle of

this silty clay layer would then correlate to the weak paleosol subunit within loess layer  $L_9$ , which corresponds to MIS 23 at ~0.89–0.92 Ma (Fig. 8E) (Heslop et al., 2000; Ding et al., 2002; Sun et al., 2006; Liu et al., 2015). The coarse and thick loess layer  $L_9$  is linked to a notably cold and arid period in North China (Heslop et al., 2000; Ding et al., 2002; Liu et al., 2015), which is possibly associated with frequent major dust events. However, the period in which the weak paleosol subunit developed within loess layer  $L_9$ , that is MIS 23, had a relatively warm interglacial climate (Heslop et al., 2000; Lisiecki and Raymo, 2005; Wu and Wu, 2011). This age estimate and associated climate inference are consistent with the hypothesis that Early Pleistocene hominins inhabited North China periodically during favorable interglacial periods (Dennell, 2009, 2013).

## 5.2. Implications for the distribution of Acheulian technology outside of Africa

Current consensus in defining a lithic assemblage to represent typical Acheulian technology depends on the following characteristic attributes: the ability to produce large flake blanks and to recurrently shape these blanks into LCTs that are typologically qualified as Acheulian tool types (i.e., handaxes, cleavers, and picks) (Isaac, 1969; Semaw et al., 2009; Stout, 2011; Beyene et al., 2013; Díez-Martín et al., 2015; Dennell, 2016). Accordingly, the technological traits (i.e., production of large flakes) and typological traits (i.e., readily attribution of LCTs as handaxes, cleavers, and picks),

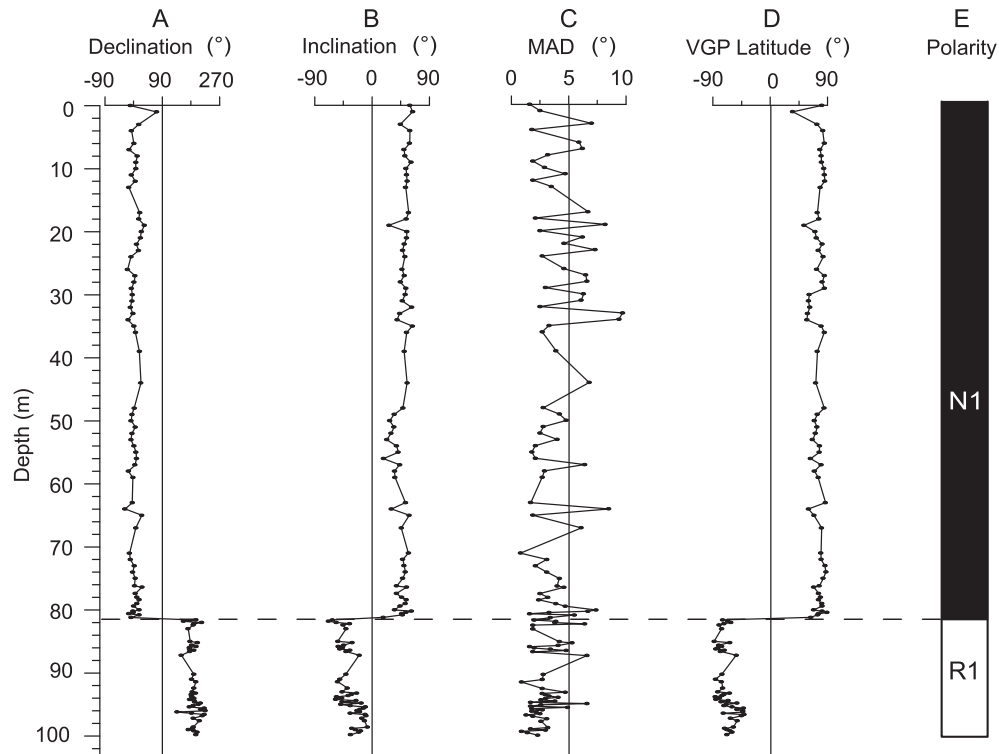


**Fig. 7.** Magnetic polarity stratigraphy of the Huixinggou section. (A) Declination; (B) Inclination; (C) maximum angular deviation (MAD); (D) virtual geomagnetic pole (VGP) latitude; and (E) magnetic polarity sequence.

which are documented in the lithic assemblage from the Shuigou-Huixinggou site, point unambiguously to Acheulian technology.

Our newly established age of ~0.9 Ma for these artefacts provides evidence for the emergence of Acheulian technology in North China as early as the late Early Pleistocene. The tools are slightly older than the Bose Acheulian stone tools, which are considered the oldest in South China and are dated at ~0.8 Ma with  $^{40}\text{Ar}/^{39}\text{Ar}$  dating of *in situ* tektites (Hou et al., 2000). Combined with 0.9–0.8 Ma ages for Acheulian stone tools from Yunxian in central China (de Lumley and Li, 2008) and from Sangiran in Indonesia (Simanjuntak et al., 2010), the Acheulian appears to have extended across a large area in East Asia since the terminal Early Pleistocene. Apparently, the hominins with this advanced technology, most likely *Homo erectus*, were adapted to diverse habitats that ranged from tropical rainforests in Indonesia to subtropical evergreen broad-leaved forests in South China, and now to temperate grasslands in North China during the late Early Pleistocene. This supports the proposition that the Movius Line (Movius, 1948) over which no Acheulian artefacts were argued to occur in East Asia is no longer an appropriate concept for the Early Paleolithic of East and Southeast Asia and should be disregarded (Hou et al., 2000; Wang, 2005; Li et al., 2014; Dennell, 2016). Although the presence of late Early Pleistocene Acheulian technology has been established firmly in East Asia, there is no consensus concerning its origin (Li et al., 2014). Some researchers interpret it to have been introduced into China with population movements from the west (Hou et al., 2000; Wang, 2005; Huang et al., 2009), while another possibility is that these Early Pleistocene Acheulian artefacts were manufactured by the descendants of hominins that left Africa earlier (Lycett and Norton, 2010).

Widespread distribution of Acheulian technology in East Asia, as documented here, is roughly coeval with their first emergence in Europe (e.g., Estrecho del Quípar and Barranc de la Boella, Spain) at ~1.0–0.9 Ma (Scott and Gibert, 2009; Vallverdú et al., 2014). By

comparison, Acheulian technology appeared in the eastern Mediterranean (e.g., ‘Ubeidiya) and South India (e.g., Attirampakkam) as early as ~1.4 Ma (Bar-Yosef and Goren-Inbar, 1993) and 1.5–1.1 Ma (Pappu et al., 2011), respectively. Combined with ~0.8–0.7 Ma Acheulian stone tools from Gesher Benot Ya’aqov (Israel) (Goren-Inbar et al., 2000), a widespread Early Pleistocene distribution of Acheulian technology outside of Africa is suggested, with expansion by ~0.9 Ma across the southern, western, and eastern portions of Eurasia, including temperate North China (Fig. 1).

### 5.3. Implications for early human occupation of North China

During the late Early Pleistocene, global climate variability shifted from lower-amplitude ~40 kyr oscillations to higher-amplitude ~100 kyr oscillations (Clark et al., 2006). This climate transition lasted from ~1.2 Ma to ~0.7 Ma (Clark et al., 2006), but occurred in North China (including the Loess Plateau) at 0.9–0.7 Ma (Heslop et al., 2002; Ao et al., 2012). Pollen data indicate mainly savanna grassland conditions on the Loess Plateau during the late Early Pleistocene (Wang et al., 2002; Wu et al., 2004). The occurrence of Acheulian tools in Sanmenxia Basin against such a global climatic and regional environmental background points to the role of climate in shaping the behavior of early humans, which is consistent with the climatic variability selection hypothesis of hominin evolution (Potts, 1998).

The southern Loess Plateau in the middle reaches of the Yellow River north of the Qinling Mountains, including Sanmenxia Basin, was an important habitat for early humans in North China. Many hominin and Paleolithic sites have been found in this region, such as the hominin sites of Gongwangling (1.63 Ma) (Zhu et al., 2015), Chenjiawo (0.65 Ma) (An and Ho, 1989), Dali (0.27 Ma) (Xiao et al., 2002) and Dingcun (0.21–0.16 Ma) (Chen et al., 1984), as well as the Paleolithic sites from Xihoudu (1.4–1.27 Ma) (Zhu et al., 2003; Kong et al., 2013), Luonan Basin (0.8–0.7, 0.4–0.3, and 0.2–0.1 Ma) (Lu



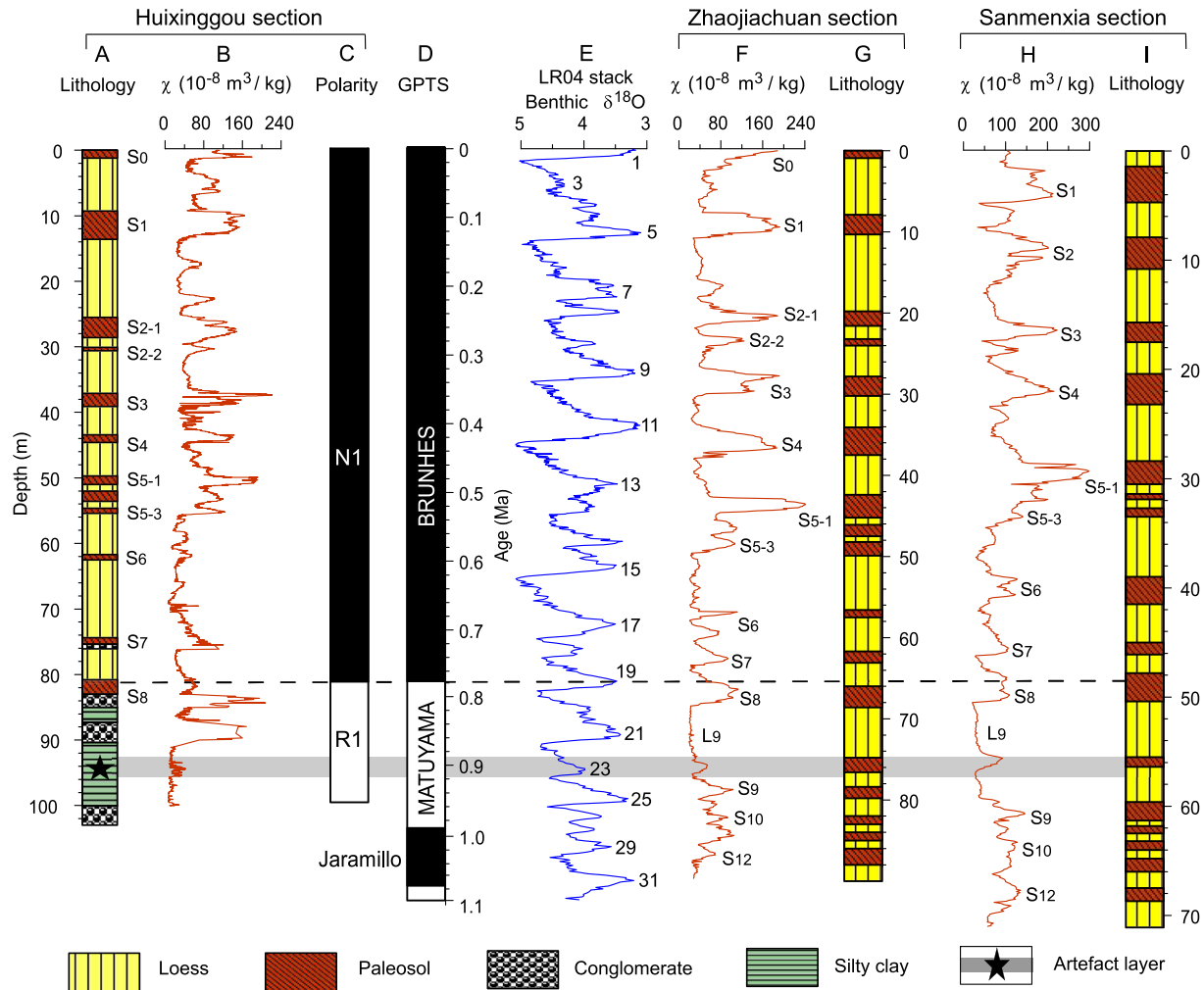


**Fig. 8.** Lithostratigraphy, magnetic susceptibility stratigraphy and magnetostratigraphy for the Huixinggou, Zhaojiachuan (Sun et al., 2006) and Sanmenxia (Wang et al., 2005) sections, and correlations to the geomagnetic polarity time scale (GPTS) (Hilgen et al., 2012) and to the LR04 stack of benthic  $\delta^{18}\text{O}$  records (Lisiecki and Raymo, 2005).

et al., 2011b), Lushi Basin (0.62–0.6 Ma) (Lu et al., 2011a), Beiyao (0.2–0.01 Ma) (Du and Liu, 2014), and the Lantian area (0.6–0.03 Ma) (Wang et al., 2014). Combined with the abundant Paleolithic sites in Nihewan Basin, North China (Ao et al., 2013a), including the oldest sites of Majuangou (1.66 Ma) (Zhu et al., 2004) and Shangshazui (1.7–1.6 Ma) (Ao et al., 2013b), there appears to have been a flourishing population of early humans in North China since the Early Pleistocene.

## 6. Conclusions

An integrated stratigraphic analysis, involving lithostratigraphy, magnetic susceptibility stratigraphy and magnetostratigraphy, indicates that the Huixinggou section records the upper Matuyama and Brunhes chrons. The Acheulian-bearing layer occurs in a reversed polarity magnetozone below the Matuyama–Brunhes boundary and is probably equivalent to MIS 23, which yields an estimated age of ~0.9 Ma. This discovery indicates that the emergence of Acheulian technology in North China can be dated back to the Early Pleistocene. Along with archeological evidence from South China and Southeast Asia, the Acheulian now appears to have been widespread in East Asia since the terminal Early Pleistocene. The East Asian occurrences of Acheulian technology are contemporaneous with the first emergence of Acheulian tools in Europe and support a wide geographic distribution of Acheulian

technology outside of Africa during the Early Pleistocene. Our results have important implications for understanding early human occupation on the Chinese Loess Plateau and provide guidance for future archeological investigations in this region.

## Acknowledgments

We are grateful to the editor Xiaoping Yang, Professors Robin W. Dennell, Gary R. Scott, and Zhaoyu Zhu for their helpful comments and suggestions on various versions of this paper, and we thank the Sanmenxia Yellow River Park and Professor Zhaoyu Zhu for assistance during fieldwork. This study was supported financially by Chinese Academy of Sciences (Youth Innovation Promotion Program and Key Research Program of Frontier Sciences), the National Natural Science Foundation of China (Grants 41420104008, 41174057, 41290250 and 41290253), the Australian Research Council (DP110105419), the International Partnership Program of Chinese Academy of Sciences (Grants 132B61KYSB20130003 and 132B61KYSB20160003), and the State Key Laboratory of Loess and Quaternary Geology at the Institute of Earth Environment, CAS (SKLLQG 1501 and 1502).

## Appendix A. Supplementary data

Supplementary data related to this article can be found at <http://>

dx.doi.org/10.1016/j.quascirev.2016.11.025

## References

- An, Z., Ho, C., 1989. New magnetostratigraphic data of Lantian *Homo erectus*. *Quat. Res.* 32, 213–221.
- An, Z., Kukla, G.J., Porter, S.C., Xiao, J., 1991. Magnetic susceptibility evidence of monsoon variation on the Loess Plateau of central China during the last 130,000 years. *Quat. Res.* 36, 29–36.
- Ao, H., An, Z., Dekkers, M.J., Li, Y., Xiao, G., Zhao, H., Qiang, X., 2013a. Pleistocene magnetochronology of the fauna and Paleolithic sites in the Nihewan Basin: significance for environmental and hominin evolution in North China. *Quat. Geochron.* 18, 78–92.
- Ao, H., Dekkers, M.J., Wei, Q., Qiang, X., Xiao, G., 2013b. New evidence for early presence of hominids in North China. *Sci. Rep.* 3, 2403. <http://dx.doi.org/10.1038/srep02403>.
- Ao, H., Dekkers, M.J., Deng, C., Zhu, R., 2009. Paleoclimatic significance of the Xiantai fluvio-lacustrine sequence in the Nihewan Basin (North China), based on rock magnetic properties and clay mineralogy. *Geophys. J. Int.* 177, 913–924.
- Ao, H., Dekkers, M.J., Xiao, G., Yang, X., Qin, L., Liu, X., Qiang, X., Chang, H., Zhao, H., 2012. Different orbital rhythms in the Asian summer monsoon records from North and South China during the Pleistocene. *Glob. Planet. Change* 80, 51–60.
- Bar-Yosef, O., Goren-Inbar, N., 1993. The Lithic Assemblages of 'Ubeidiya: a Lower Palaeolithic Site in the Jordan Valley, Jerusalem. The Hebrew University of Jerusalem, Jerusalem.
- Beysen, Y., Katoh, S., WoldeGabriel, G., Hart, W.K., Uto, K., Sudo, M., Kondo, M., Hyodo, M., Renne, P.R., Suwa, G., Asfaw, B., 2013. The characteristics and chronology of the earliest Acheulean at Konso, Ethiopia. *Proc. Natl. Acad. Sci. U. S. A.* 110, 1584–1591.
- Chen, T., Yuan, S., Gao, S., 1984. The study on uranium-series dating of fossil bones and an absolute age sequence for the main Paleolithic sites of North China. *Acta Anthropol. Sin.* 3, 259–269 (in Chinese with English abstract).
- Clark, P.U., Archer, D., Pollard, D., Blum, J.D., Rial, J.A., Brovkin, V., Mix, A.C., Piasis, N.G., Roy, M., 2006. The middle Pleistocene transition: characteristics, mechanisms, and implications for long-term changes in atmospheric  $\mu\text{CO}_2$ . *Quat. Sci. Rev.* 25, 3150–3184.
- de Lumley, H., Li, T., 2008. Le site de L'Homme de Yunxian. CNRS Éditions Recherche sur les Civilisations, Paris.
- Deng, C., Zhu, R., Verosub, K.L., Singer, M.J., Vidic, N.J., 2004. Mineral magnetic properties of loess/paleosol couplets of the central loess plateau of China over the last 1.2 Myr. *J. Geophys. Res.* 109, B01103. <http://dx.doi.org/10.1029/2003JB002532>.
- Deng, C., Shaw, J., Liu, Q., Pan, Y., Zhu, R., 2006. Mineral magnetic variation of the Jingbian loess/paleosol sequence in the northern Loess Plateau of China: implications for Quaternary development of Asian aridification and cooling. *Earth Planet. Sci. Lett.* 241, 248–259.
- Dennell, R.W., 2009. The Palaeolithic Settlement of Asia. Cambridge University Press, Cambridge.
- Dennell, R.W., 2013. The Nihewan Basin of North China in the early Pleistocene: continuous and flourishing, or discontinuous, infrequent and ephemeral occupation? *Quat. Int.* 295, 223–236.
- Dennell, R.W., 2016. Life without the Movius line: the structure of the east and Southeast Asian Early Palaeolithic. *Quat. Int.* 400, 14–22.
- Díez-Martín, F., Sánchez Yustos, P., Uribealrrea, D., Baquedano, E., Mark, D.F., Mabulla, A., Fraile, C., Duque, J., Díaz, I., Pérez-González, A., Yravedra, J., Egeland, C.P., Organista, E., Domínguez-Rodrigo, M., 2015. The origin of the Acheulean: the 1.7 million-year-old site of FLK west, Olduvai Gorge (Tanzania). *Sci. Rep.* 5, 17839. <http://dx.doi.org/10.1038/srep17839>.
- Ding, Z., Derbyshire, E., Yang, S., Yu, Z., Xiong, S., Liu, T., 2002. Stacked 2.6-Ma grain size record from the Chinese loess based on five sections and correlation with the deep-sea  $\delta^{18}\text{O}$  record. *Paleoceanography* 17, 1033. doi: 10.1029/2001PA000725.
- Du, S., Liu, F., 2014. Loessic palaeolith discovery at the Beiyao site, Luoyang, and its implications for understanding the origin of modern humans in Northern China. *Quat. Int.* 349, 308–315.
- Florindo, F., Zhu, R., Guo, B., Yue, L., Pan, Y., Speranza, F., 1999. Magnetic proxy climate results from the Duanjiapo loess section, southernmost extremity of the Chinese loess plateau. *J. Geophys. Res.* 104 (B1), 645–659.
- Gibbon, R.J., Granger, D.E., Kuman, K., Partridge, T.C., 2009. Early Acheulean technology in the Rietputs Formation, South Africa, dated with cosmogenic nuclides. *J. Hum. Evol.* 56, 152–160.
- Goren-Inbar, N., 2011. Culture and cognition in the Acheulean industry: a case study from Gesher Benot Ya'aqov. *Philos. Trans. R. Soc. Lond. B* 366, 1038–1049.
- Goren-Inbar, N., Feibel, C.S., Verosub, K.L., Melamed, Y., Kislev, M.E., Tchernov, E., Saragusti, I., 2000. Pleistocene milestones on the out-of-Africa corridor at Gesher Benot Ya'aqov, Israel. *Science* 289, 944–947.
- Heller, F., Liu, T., 1982. Magnetostratigraphical dating of loess deposits in China. *Nature* 300, 161–163.
- Heslop, D., Dekkers, M.J., Langereis, C.G., 2002. Timing and structure of the mid-Pleistocene transition: records from the loess deposits of northern China. *Palaeogeogr. Palaeoclimatol. Palaeoecol.* 185, 133–143.
- Heslop, D., Langereis, C.G., Dekkers, M.J., 2000. A new astronomical timescale for the loess deposits of Northern China. *Earth Planet. Sci. Lett.* 184, 125–139.
- Hilgen, F.J., Lourens, L.J., van Dam, J.A., 2012. The neogene period. In: Gradstein, F.M., Ogg, J.G., Schmitz, M., Ogg, G. (Eds.), *The Geologic Time Scale*. Elsevier, pp. 923–978.
- Hou, Y., Potts, R., Yuan, B., Guo, Z., Deino, A., Wang, W., Clark, J., Xie, G., Huang, W., 2000. Mid-Pleistocene Acheulean-like stone technology of the Bose basin, South China. *Science* 287, 1622–1626.
- Huang, W., 1964. On a collection of Palaeoliths from Sanmen area in western Honan. *Vertebr. Palasiat.* 8, 162–177 (in Chinese with English abstract).
- Huang, W., 1987. Bifaces in China. *Acta Anthropol. Sin.* 6, 61–68 (in Chinese with English abstract).
- Huang, W., 1993. On the typology of heavy-duty tools of the lower Paleolithic from East and Southeast Asia—comment on the Movius' system. *Acta Anthropol. Sin.* 12, 297–304 (in Chinese with English abstract).
- Huang, W., Hou, Y., Gao, L., 2009. "Western elements" in the Chinese Paleolithic as viewed in a framework of early human cultural evolution. *Acta Anthropol. Sin.* 28, 16–25 (in Chinese with English abstract).
- Huang, W., Hou, Y., Seong, H., 2005. The pebble-tool tradition in China. *Archaeol. Ethnol. Anthropol. Eur.* 1, 2–15.
- Hunt, C.P., Banerjee, S.K., Han, J., Solheid, P.A., Oches, E., Sun, W., Liu, T., 1995. Rock-magnetic proxies of climate change in the loess-paleosol sequences of the western Loess Plateau of China. *Geophys. J. Int.* 123, 232–244.
- Isaac, G.L., 1969. Studies of early culture in East Africa. *World Archaeol.* 1, 1–28.
- Jia, L., 1985. China's earliest Paleolithic industries. In: Wu, R., Olsen, J.W. (Eds.), *Palaeoanthropology and Paleolithic Archaeology in the People's Republic of China*. Academic Press, New York, pp. 134–135.
- Jia, L., Wang, Z., Qiu, Z., 1961. Palaeoliths in Shansi. *Science Press, Beijing*, pp. 1–48 (in Chinese).
- Kirschvink, J.L., 1980. The least-squares line and plane and the analysis of palaeomagnetic data. *Geophys. J. R. Astron. Soc.* 62, 699–718.
- Kong, P., Jia, J., Zheng, Y., 2013. Cosmogenic  $^{26}\text{Al}/^{10}\text{Be}$  burial dating of the Paleolithic at Xihoudu, North China. *J. Hum. Evol.* 64, 466–470.
- Kukla, G., An, Z., 1989. Loess stratigraphy in central China. *Palaeogeogr. Palaeoclimatol. Palaeoecol.* 72, 203–225.
- Kukla, G., Heller, F., Liu, X., Xu, T., Liu, T., An, Z., 1988. Pleistocene climates in China dated by magnetic susceptibility. *Geology* 16, 811–814.
- Lepre, C.J., Roche, H., Kent, D.V., Harmand, S., Quinn, R.L., Brugal, J.P., Texier, P.J., Lenoble, A., Feibel, C.S., 2011. An earlier origin for the Acheulean. *Nature* 477, 82–85.
- Li, H., Li, C., Kuman, K., 2014. Rethinking the "Acheulean" in East Asia: evidence from recent investigations in the Danjiangkou Reservoir region, central China. *Quat. Int.* 347, 163–175.
- Li, Z., 1990. A preliminary report on the excavation of the Yingli Paleolithic locality in the Lingbao, Henan. *Huaxia Archaeol.* 2, 1–8 (in Chinese with English abstract).
- Lin, S., 1992. Cleavers in China. *Acta Anthropol. Sin.* 11, 193–201 (in Chinese with English abstract).
- Lisiecki, L.E., Raymo, M.E., 2005. A Pliocene-Pleistocene stack of 57 globally distributed benthic  $\delta^{18}\text{O}$  records. *Paleoceanography* 20, PA1003. doi: 10.1029/2004PA001071.
- Liu, Q., Deng, C., Yu, Y., Torrent, J., Jackson, M.J., Banerjee, S.K., Zhu, R., 2005. Temperature dependence of magnetic susceptibility in argon environment: implications for pedogenesis of Chinese loess/paleosols. *Geophys. J. Int.* 161, 102–112.
- Liu, Q., Jin, C., Hu, P., Jiang, Z., Ge, K., Roberts, A.P., 2015. Magnetostratigraphy of Chinese loess-paleosol sequences. *Earth-Sci. Rev.* 150, 139–167.
- Liu, T., 1985. Loess and the Environment. China Ocean Press, Beijing.
- Lu, H., Sun, X., Wang, S., Cosgrove, R., Zhang, H., Yi, S., Ma, X., Wei, M., Yang, Z., 2011a. Ages for hominin occupation in Lushi Basin, middle of South Luo River, central China. *J. Hum. Evol.* 60, 612–617.
- Lu, H., Zhang, H., Wang, S., Cosgrove, R., Sun, X., Zhao, J., Sun, D., Zhao, C., Shen, C., Wei, M., 2011b. Multiphase timing of hominin occupations and the paleo-environment in Luonan Basin, Central China. *Quat. Res.* 76, 142–147.
- Lycett, S., Norton, C., 2010. A demographic model for Palaeolithic technological evolution: the case of East Asia and the Movius Line. *Quat. Int.* 211, 55–65.
- May, S.R., Butler, R.F., 1986. North American Jurassic apparent polar wander: implications for plate motion, paleogeography and Cordilleran Tectonics. *J. Geophys. Res.* 91, 1519–1544.
- McFadden, P.L., McElhinny, M.W., 1990. Classification of the reversal test in palaeomagnetism. *Geophys. J. Int.* 103, 725–729.
- Movius, H.L., 1948. The lower Palaeolithic cultures of southern and eastern Asia. *Trans. Am. Philos. Soc.* 38, 329–420.
- Pan, B., Wang, J., Gao, H., Chen, Y., Li, J., Liu, X., 2005. Time of the Yellow River flowing eastwards to sea based on age of the river terraces near the Sanmen Gorge. *Prog. Nat. Sci.* 15, 700–705 (in Chinese).
- Pappu, S., Gunnell, Y., Akhilesh, K., Braucher, R., Taieb, M., Demory, F., Thouveny, N., 2011. Early Pleistocene presence of Acheulean hominins in South India. *Science* 331, 1596–1599.
- Porter, S.C., An, Z., 1995. Correlation between climate events in the North Atlantic and China during the last glaciation. *Nature* 375, 305–308.
- Potts, R., 1998. Environmental hypotheses of Hominin evolution. *Yearb. Phys. Anthropol.* 41, 93–136.
- Roberts, A.P., 2008. Geomagnetic excursions: knowns and unknowns. *Geophys. Res. Lett.* 35, L17307. doi: 10.1029/2008GL034719.
- Scott, G.R., Gibert, L., 2009. The oldest hand-axes in Europe. *Nature* 461, 82–85.
- Semaw, S., Rogers, M., Stout, D., 2009. The Oldowan-Acheulean transition: is there a "Developed Oldowan" artifact tradition? In: Camps, M., Chauhan, P. (Eds.),

- Sourcebook of Paleolithic Transitions. Springer, New York, pp. 173–192.
- Simanjuntak, T., Semah, F., Gaillard, C., 2010. The palaeolithic in Indonesia: nature and chronology. *Quat. Int.* 223, 418–421.
- Stout, D., 2011. Stone toolmaking and the evolution of human culture and cognition. *Philos. Trans. R. Soc. Lond. B* 366, 1050–1059.
- Sun, Y., Clemens, S.C., An, Z., Yu, Z., 2006. Astronomical timescale and palaeoclimatic implication of stacked 3.6-Myr monsoon records from the Chinese Loess Plateau. *Quat. Sci. Rev.* 25, 33–48.
- Vallverdú, J., Saladié, P., Rosas, A., Huguet, R., Cáceres, I., Mosquera, M., García-Tabernero, A., Estalrich, A., Lozano-Fernández, I., Pineda-Alcalá, A., Carrancho, A., Villalain, J.J., Bourlès, D., Braucher, R., Lebatard, A., Vilalta, J., Esteban-Nadal, M., Bennàsar, M.L., Bastir, M., López-Polín, L., Ollé, A., Vergés, J.M., Ros-Montoya, S., Martínez-Navarro, B., García, A., Martinell, J., Expósito, I., Burjachs, F., Agustí, J., Carbonell, E., 2014. Age and Date for Early Arrival of the Acheulian in Europe (Barranc de la Boella, la Canonja, Spain). *PLoS One* 9, e103634. <http://dx.doi.org/10.1371/journal.pone.0103634>.
- Wang, S., 2005. Perspectives on hominid behaviour and settlement patterns: a study of the Lower Palaeolithic sites in the Luonan Basin, China. In: *British Archaeological Reports International Series 1406*. Archaeopress, Oxford.
- Wang, S., Jiang, F., Wu, X., Wang, S., Tian, G., 2004. The connotation and significance of Sanmen formation. *Quat. Sci.* 21, 116–123 (in Chinese with English abstract).
- Wang, S., Lu, H., Zhang, H., Sun, X., Yi, S., Chen, Y., Zhang, G., Xing, L., Sun, W., 2014. Newly discovered Palaeolithic artefacts from loess deposits and their ages in Lantian, central China. *Sci. Bull.* 59, 651–661.
- Wang, S., Wu, X., Zhang, Z., Jiang, F., Xue, B., Tong, G., Tian, G., 2002. Sedimentary records of environmental evolution in the Sanmen Lake Basin and the Yellow River running through the Sanmenxia Gorge eastward into the sea. *Sci. China Earth Sci.* 47, 595–608.
- Wang, X., Løvlie, R., Yang, Z., Pei, J., Zhao, Z., Sun, Z., 2005. Remagnetization of quaternary eolian deposits: a case study from SE Chinese Loess Plateau. *Geochem. Geophys. Geosyst.* 6 <http://dx.doi.org/10.1029/2004GC000901>. Q06H18.
- Wu, B., Wu, N., 2011. Terrestrial mollusc records from Xifeng and Luochuan L9 loess strata and the implications for paleoclimatic evolution in the Chinese Loess Plateau during marine oxygen isotope stages 24–22. *Clim. Past.* 7, 349–359.
- Wu, F., Fang, X., Ma, Y., An, Z., Li, J., 2004. A 1.5 Ma sporopollen record of paleo-ecologic environment evolution in the central Chinese Loess Plateau. *Sci. Bull.* 49, 295–302.
- Xiao, J., Jin, C., Zhu, Y., 2002. Age of the fossil Dali Man in north-central China deduced from chronostratigraphy of the loess-paleosol sequence. *Quat. Sci. Rev.* 21, 2191–2198.
- Yang, S., Huang, W., Hou, Y., Yuan, B., 2014. Is the Dingcun lithic assembly a “chopper-chopping tool industry”, or “Late Acheulian”? *Quat. Int.* 321, 3–11.
- Young, C., Pei, W., 1933. The cenozoic geology between Luoyang and Xi'an. *Bull. Geol. Soc. China* 13, 73–90.
- Zhu, R., An, Z., Potts, R., Hoffman, K.A., 2003. Magnetostratigraphic dating of early humans in China. *Earth Sci. Rev.* 61, 341–359.
- Zhu, R., Deng, C., Jackson, M.J., 2001. A magnetic investigation along a NW-SE transect of the Chinese Loess Plateau and its implications. *Phys. Chem. Earth A* 26, 867–872.
- Zhu, R., Potts, R., Xie, F., Hoffman, K.A., Deng, C., Shi, C., Pan, Y., Wang, H., Shi, R., Wang, Y., Shi, G., Wu, N., 2004. New evidence on the earliest human presence at high northern latitudes in northeast Asia. *Nature* 431, 559–562.
- Zhu, Z., Dennell, R.W., Huang, W., Wu, Y., Rao, Z., Qiu, S., Xie, J., Liu, W., Fu, S., Han, J., Zhou, H., Ouyang, T., Li, H., 2015. New dating of the *Homo erectus* cranium from Lantian (Gongwangling), China. *J. Hum. Evol.* 78, 144–157.
- Zijderveld, J.D.A., 1967. AC demagnetization of rocks: analysis of results. In: Collinson, D.W., Creer, K.M., Runcorn, S.K. (Eds.), *Methods in Paleomagnetism*. Elsevier, New York, pp. 254–286.